ACADEMIA ROMÂNĂ
Revue Roumaine de Chimie
http://web.icf.ro/rrch/

Rev. Roum. Chim.,
2016, *61*(2), 105-110

SYNTHESIS OF SILVER SECONDARY SHELL MAGNETIC NANOPARTICLES

Dan E. MIHAIESCU,[a] Dragos GUDOVAN,[a] Vanessa TRAISTARU,[b] Paul IONESCU,[c] Adrian FUDULU,[c] Georgeta VOICU,[b] Anton FICAI,[b] Roxana TRUŞCĂ,[d] Daniela ISTRATI,[a,*] Anca MARTON,[a] Sandra Alice BUTEICA,[e] Bogdan VASILE[b] and Ecaterina ANDRONESCU[b]

[a] "Costin Nenitescu" Department of Organic Chemistry, Faculty of Applied Chemistry and Materials Science, Politehnica University of Bucharest, 1-7 Polizu Street, 011061 Bucharest, Roumania
[b] Department of Science and Engineering of Oxide Materials and Nanomaterials, Faculty of Applied Chemistry and Materials Science, Politehnica University of Bucharest, 1-7 Polizu Street, 011061 Bucharest, Roumania
[c] Department of Inorganic Chemistry, Physical Chemistry and Electrochemistry, Faculty of Applied Chemistry and Materials Science, Politehnica University of Bucharest, 1-7 Polizu Street, 011061 Bucharest, Roumania
[d] Metav Research-Development srl, 31 C.A. Rosetti Street, Bucharest 020011 Roumania
[e] Drug Control Department, Faculty of Pharmacy, University of Medicine and Pharmacy of Craiova, 2 Petru Rareş Street, 200349 Roumania

Received October 30, 2015

In this paper we present the synthesis of magnetic core nanoparticles with a multishell structure: para-aminobenzoic acid as a primary shell, silver as a secondary shell and para-aminobenzoic acid as a final organic shell. The intermediate and final nanoparticles are water dispersible due to the polar organic shell. The purpose of the silver secondary shell is to reduce the consumption of silver and other noble metals for the synthesis of similar nanoparticles. Para-aminobenzoic acid was chosen as a shell due to the fact that it provides a good water dispersability of the final nanoparticles. The magnetic properties of the Fe_3O_4 core are useful in all purification stages, by using magnetic separation. The obtained materials were characterized by UV-VIS, XRD, FT-IR and TEM.

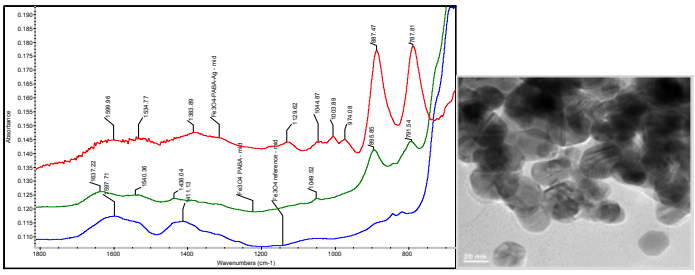

INTRODUCTION

Nanosized metal particles have been a subject of intensive research, due to their unique physical, chemical and biological properties leading to a wide range of applications in biomedicine,[1] catalysis,[2] sensors,[3] energy conversion,[4] tissue imaging,[5] targeted drug delivery.[6,7] The incorporation of magnetic components into silver nanoparticles-based catalysts[8] enhances the separation and recovery of nanosized silver. Due to their reduced size, nanoparticles (NPs) behave as super-paramagnets[9] *i.e.* the magnetization curves versus applied magnetic field can be fitted with Langevin function and do not present hysteresis.[10] NPs do not behave as conventional bulk ferromagnets[11] they can be guided by a static magnetic field within the human body allowing, for instance, specific drug delivery.[12] Contrary to bulk ferromagnets[13] once the field is removed, the absence of magnetic remanence

* Corresponding author: d_istrati@yahoo.com, 0724351487

prevents problems associated to particle aggregation. Silver NPs are well-known for their bactericidal effect[14] based on the release of silver ions.[15, 16] There are many synthetic routes that have been reported to synthesize Fe_3O_4-Ag nanoparticles, including a solvothermal method,[17] hydrothermal process,[18] thermal decomposition,[19] two-step chemical method.[20] Various shapes of silver NPs have been synthesized, among which, brick shaped Ag@Fe_3O_4 NPs with a larger shell-to-core ratio and compact structure.[21] The compact cubic magnetic shell could potentially solve the lack of biocompatibility of silver.[22] These brick-like NPs can represent a significant advance for in-vivo applications of silver-magnetite heterodimers.[23, 24] Another novel synthesis route is the biogenic synthesis of Fe_3O_4-Ag core shell NPs. It's considered a green method due to the fact that it uses an aqueous stem extract of *Vitisvinifera* (a by-product of the *V.vinifera* and wine industry), and no hazardous chemicals as solvent and reducing and stabilizing agent during synthesis.

In this paper we synthesized Fe_3O_4 core shell nanoparticles with a primary para-aminobenzoic acid shell, silver secondary shell and para-aminobenzoic acid as final organic shell.

RESULTS AND DISCUSSION

A convenient synthetic route for silver / PABA secondary shell nanoparticles production was developed, in order to obtain water dispersible nanomaterials with reduced silver consumption. It is well known that noble metal consumption is an important limitative factor in Ag, Au, Pd, Pt and other core-shell nanoparticle applications, thus this method is a good choice regarding this aspect. The magnetic core of the obtained nanoparticles offers other advantages, linked to facile magnetic separation of the intermediate materials during the whole synthetic route and possible applications in magnetic drug targeting, hyperthermia applications, magnetic assisted thin film deposition and other applications involving magnetic field – magnetic nanoparticle interactions.

The obtained silver-coated nanoparticles are expected to behave in a similar manner (certainly related only to the external shell-dispersion environment interaction) to classic full-core silver nanoparticles, with the same external organic shell (core-shell Ag/PABA NPs were synthesized using a similar method and used as reference for the UV-VIS analysis). An important experimental evidence is related to the obtained SPR (Surface Plasmon Resonance) spectra (Fig. 1). SPR peak at 409.34 nm for Fe_3O_4 / PABA / Ag / PABA nanoparticles proves that a thin silver film deposited over the classic magnetite / PABA nanoparticles, can yield almost similar spectral response as full-core silver NPs (403.09 nm), due to the surface free electrons' oscillation driven by the external electromagnetic radiation at resonance wavelength. These results prove that SPR is essentially a near-surface effect observable in thin silver films deposited on Fe_3O_4 carrier nanoparticles (this conclusion is significant considering the 20-40 nm NPs diameter and a 2-5 nm estimated Ag shell thickness).

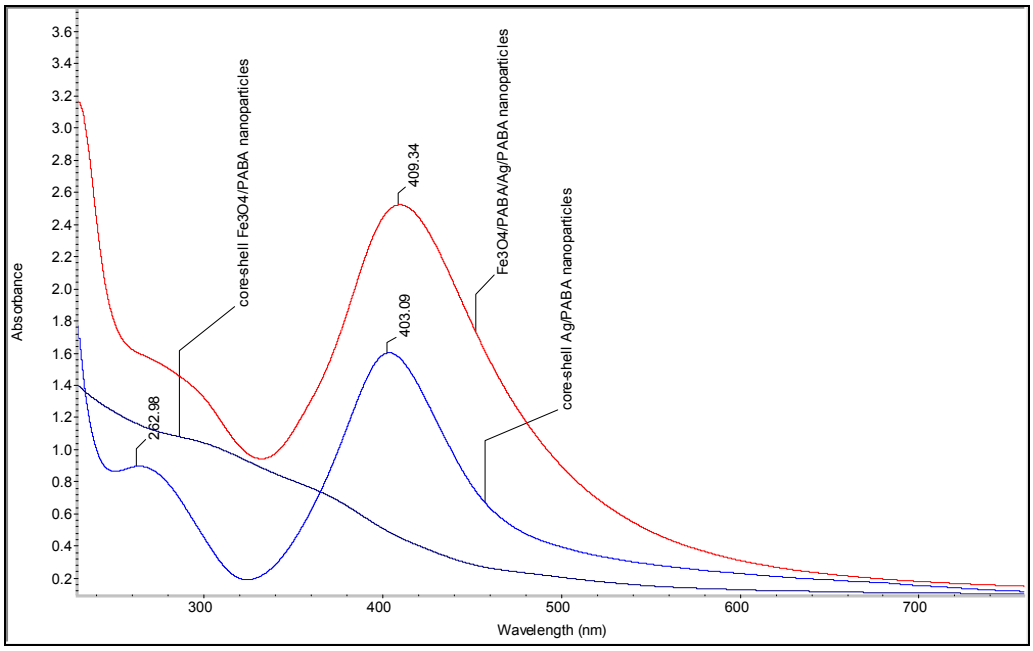

Fig. 1 – UV-VIS spectra for Ag / PABA, Fe_3O_4 / PABA and Fe_3O_4 / PABA / Ag / PABA NPs.

XRD analysis was carried out on the samples obtained through coprecipitation (Fig. 2). All the characteristic peaks of the Fe_3O_4 crystallographic phase were also identified in our sample, and the identification was made based on the PDF database. The peaks corresponding to the silver phase were noted (Fig. 5), however a change in the background noise and the extremely broad and noisy peak shape reveals the rather amorphous silver phase. The FT-IR spectroscopy (Fig. 3) reveals the presence of the p-aminobenzoic acid, the shell covering the Fe_3O_4 nanoparticles (as established in our previous work)[25] the IR shell peaks are widened due to a core lattice - shell vibrational coupling). The TEM image (Fig. 4) reveals relatively uniform particle size between 10-15 nm, clustered due to the magnetic aggregation. The same wavelengths corresponding to the vibration in the p-aminobenzoic acid's vibrational fingerprint are present also in the spectra of the nanoparticles with silver secondary shell (Fig. 6). A significant enhancement related to aromatic ring absorption peaks at 895.85 and 791.54 cm^{-1} (the out-of-plane aromatic ring C-H bending of the of the secondary PABA shell), for the silver coated NPs compared with reference Fe_3O_4 / PABA NPs, was correlated with the polarizability changes caused by Ag – external PABA shell interaction. TEM image of the Fe_3O_4 / PABA / Ag / PABA nanoparticles (Fig. 7) also show darkened interference regions of the silver shell crystalline planes with the Fe_3O_4 core crystalline structure. The size of the nanoparticles according to TEM is slightly higher, around 30 nm, which is to be expected given the secondary shell that is added to the first.

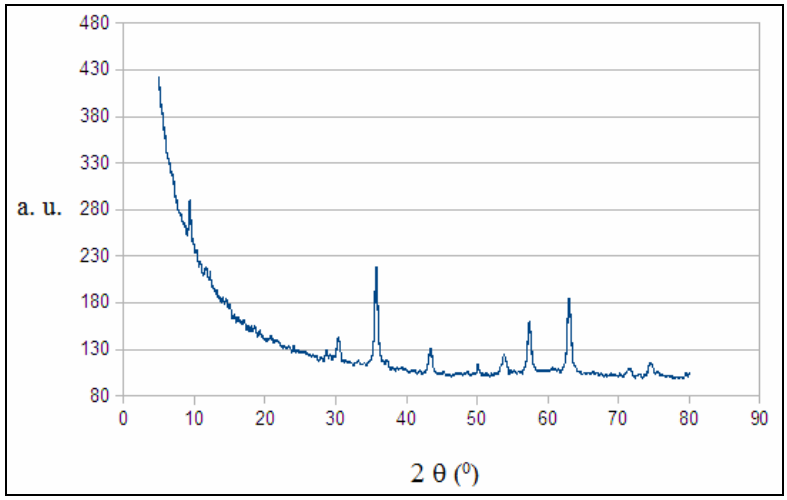

Fig. 2 – XRD for Fe_3O_4 / PABA.

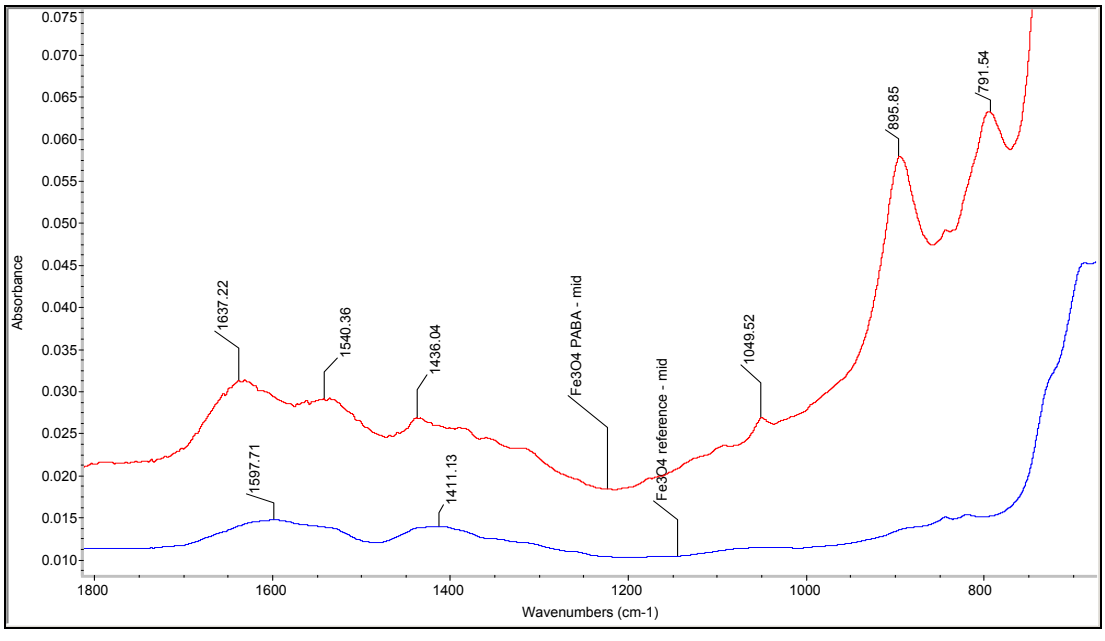

Fig. 3 – FT-IR spectrum for Fe_3O_4 and Fe_3O_4 / PABA.

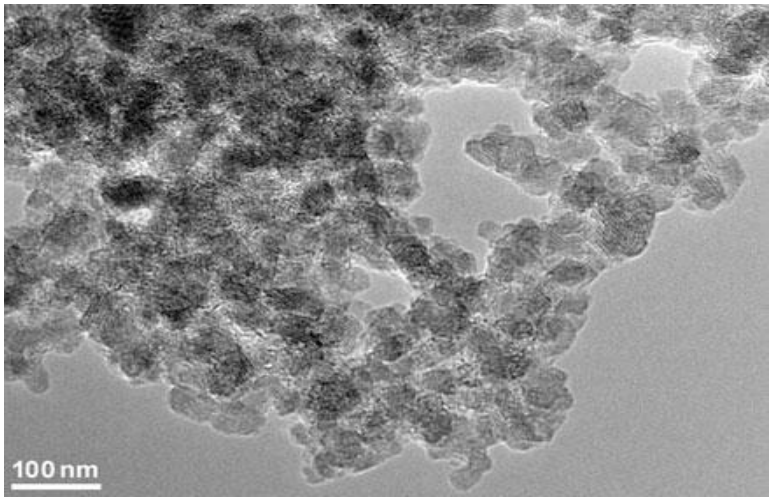

Fig. 4 – TEM images for Fe_3O_4 / PABA.

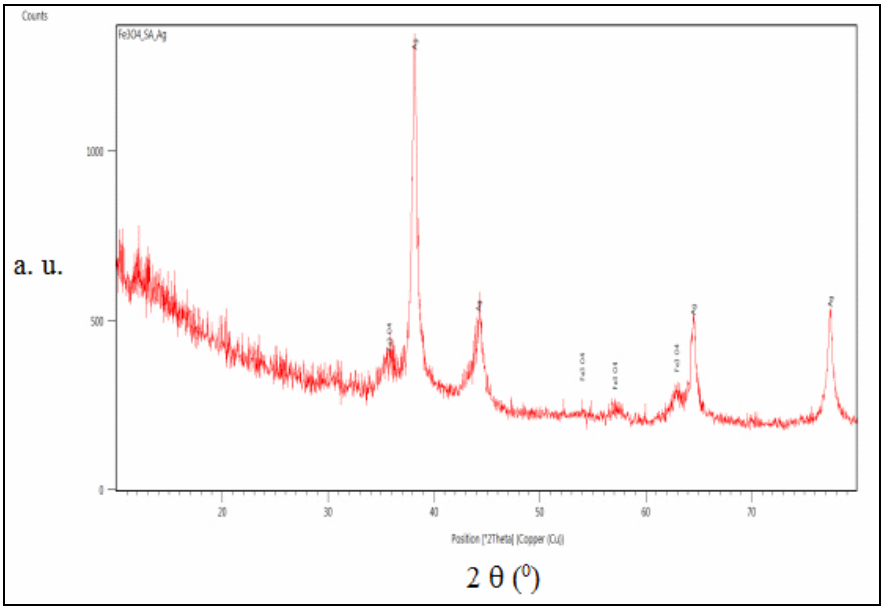

Fig. 5 – XRD for Fe_3O_4 / PABA / Ag / PABA.

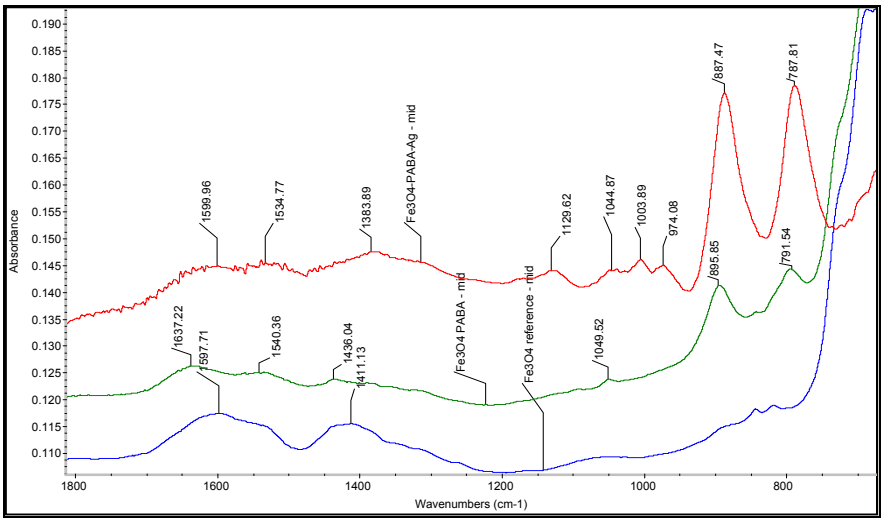

Fig. 6 – FT-IR spectrum for Fe_3O_4 ; Fe_3O_4 / PABA and Fe_3O_4 / PABA / Ag / PABA.

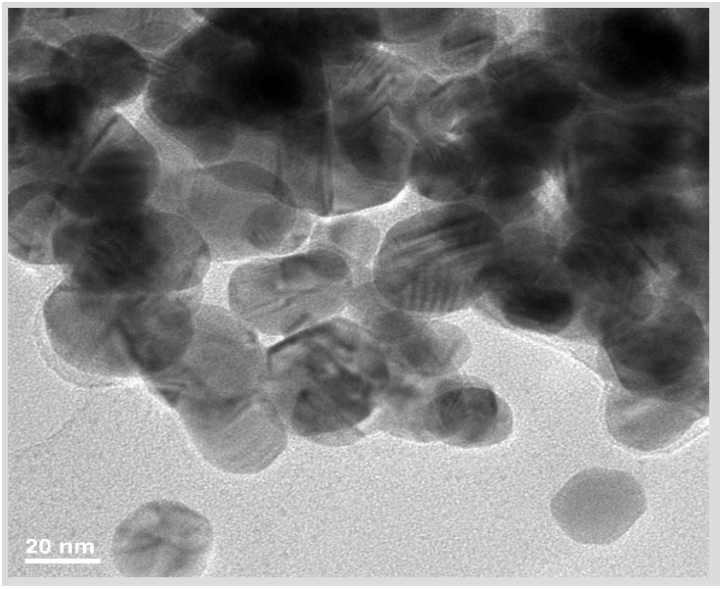

Fig. 7 – TEM images for Fe_3O_4 / PABA / Ag / PABA.

EXPERIMENTAL

The materials used for the experiments were analytical grade. PABA, $FeCl_3$, and $AgNO_3$ were purchased from Merck, CH_3COOH was purchased from Chimopar and $FeSO_4 \cdot 7H_2O$ and NaOH from Sigma-Aldrich. Ultrapure water was used in all synthetic steps. In this experiment we used as starting materials two stoichiometrically equivalent solutions of Fe^{2+} and Fe^{3+} salt solutions that coprecipitate with NaOH and para-aminobenzoic acid (PABA) under slow dripping and magnetic stirring (this modified method was based on our previously developed methods).[25]

Coprecipitation was followed by several washes and magnetic separations. Finally, we obtained a dispersion of Fe_3O_4 with PABA as primary shell. Secondary shell synthesis was carried out by the reduction of silver nitrate with glucose on the surface of water dispersed Fe_3O_4 nanoparticles, in an alkaline shell compound containing environment, under magnetic stirring. This step was followed by several washes and magnetic separations.

FT-IR spectra were carried out on a Thermo Scientific Nicolet™ iS™50 FT-IR Spectrometer with a Polaris™ long-life IR source, Tungsten-Halogen white light source, built-in mid- and far-IR diamond ATR module, NIR with Integrating Sphere and Raman module. The FT-IR spectrum was recorded using diamond ATR, in the 100-1950 cm^{-1} range.

The transmission electron images were obtained on finely powdered samples using a Tecnai^{TM} G^2 F30S-TWIN high resolution transmission electron microscope (HR-TEM) equipped with STEM—HAADF detector. The microscope was operated in transmission mode at 300 kV while TEM point resolution was 2 Å and line resolution was 1 Å.

X-ray diffraction was carried out on a PANalytical Empyrean equipment which uses CuK_α radiation (1.541874), equipped with programmable divergence slit on the incidence side and a programmable anti-scatter slit mounted on PIXcel3D detector on the diffracted side. The scan was done by using Bragg Brentanno geometry with a step size of 0.02° and a counting time per step of 100 s in the range of 2θ=20-70°.

UV-VIS analysis was carried out on a Thermo Scientific Evolution 220 UV-Visible with continuous Xe source. The measuring range was between 190-900 nm, the scanning speed used was 120 nm/min and integration time 0.45 s. Analysis was carried out in 1 cm quartz cells.

CONCLUSIONS

In this paper we described the synthesis of new silver secondary shell magnetic nanoparticles using a coprecipitation method. In the first step of synthesis, stable water dispersions of Fe_3O_4 / PABA NPs were obtained. After several washes and magnetic separations, secondary silver shell synthesis was carried out by adding silver nitrate and glucose, using PABA as a final organic shell compound. Through silver reduction, a silver coating of the primary NPs was obtained. Stable water dispersions of Fe_3O_4 / PABA / Ag / PABA nanoparticles were obtained after several purification steps and a final water dispersion. The materials were characterized by UV-VIS, XRD, FT-IR and TEM. These types of nanoparticles could potentially be used for obtaining transparent conducting materials, in photovoltaic cells research field and for various applications in biomedicine.

Acknowledgements: The participation of Vanessa Traistaru has been funded by the Sectoral Operational Programme Human Resources Development 2007- 2013 of the Ministry of European Funds through the Financial Agreement POSDRU/159/1.5/S/134398. The participation of S. A. Buteică was supported by the Project "Excellence program for multidisciplinary doctoral and postdoctoral research in chronic diseases", Grant No. POSDRU/159/1.5/S/133377, partially supported by the Sectoral Operational Programme Human

Resources Development 2007–2013, financed from the European Social Fund.

REFERENCES

1. Y.L. Zhou, Y.B. Zhang, G.H. Li, Y.D. Wu and T. Jiang, *Powder Technol.*, **2015**, *271*, 155.
2. J. Yang, L. Si, S.H. Cui and W.T. Bi, *Microchim. Acta*, **2015**, *182*, 737.
3. I.Y. Toth, E. Illes, M. Szekeres and E. Tombacz, *J. Magn. Magn. Mater*., **2015**, *308*, 168.
4. X.Y. Du, J. He, J. Zhu, L.J. Sun and S.S. An., *Appl. Surf. Sci*., **2012**, *258*, 2717.
5. Z.C. Xu, Y.L. Hou and S.H. Sun, *J. Amer. Chem. Soc*., **2007**, *129*, 8698.
6. X.Y. Yang, X.Y. Zhang, Y.F. Ma, Y. Huang, Y.S. Wang and Y.S. Chen, *J. Mater. Chem*., **2009**, *19*, 2710.
7. Q. Yu, A. Fu, H. Li, H. Liu, R. Lv, J. Liu, Peizhi Guo and X.S. Zhao, *Colloids Surf.*, *A*, **2014**, *457*, 288.
8. A.A. Babaei, Z. Baboli, N. Jaafarzadeh, G. Goudarzi, M. Bahrami and M. Ahmadi, *Desalin Water Treat*, **2015**, *53*, 768.
9. T.S. Anirudhan and F. Shainy, *J. Colloid Interface Sci*., **2015**, *456*, 22.
10. C.F. Adams, A. Rai, G. Sneddon, H.H.P. Yiu, B. Polyak and D.M. Chari, *Nanomedicine: NBM*, **2015**, *11*, 19.
11. R.D. Alorro, N. Hiroyoshi, H. Kijitani, M. Ito and M. Tsunekawa, *Miner. Process. Extr. Metall. Rev*., **2015**, *36*, 332.
12. S. Abaci, B. Nessark, R. Boukherroub and K. Lmimouni, *Thin Solid Films*, **2011**, *519*, 3596.
13. X.Q. Jiang, S. Setodoi, S. Fukumoto, I. Imae, K. Komaguchi, J. Yano, H. Mizota and Y. Harima, *Carbon*, **2014**, *67*, 662.
14. J.Y. Liu, D.A. Sonshine, S. Shervani and R.H. Hurt, *ACS Nano*, **2010**, *4*, 6903.
15. J.R. Morones, J.L. Elechiguerra, A. Camacho, K. Holt, J.B. Kouri, J.T. Ramirez and M.J. Yacaman, *Nanotechnology*, **2005**, *16*, 346.
16. G.A. Sotiriou and S.E. Pratsinis, *Environ. Sci. Technol*., **2010**, *44*, 5649.
17. B. Tutunaru, A. Samide, A. Ciuciu and M. Preda, *Stud U Babes Bol Che*, **2010**, *55*, 13.
18. R. Bernardie, S. Valette, J. Absi and P. Lefort, *Surf. Coat. Technol*., **2015**, *276*, 677.
19. B. Chudasama, A.K. Vala, N. Andhariya, R.V. Upadhyay and R.V. Mehta, *J. Magn. Magn. Mater.*, **2011**, *323*, 1233.
20. G. Lopes, J.M. Vargas, S.K. Sharma, F. Beron, K.R. Pirota, M. Knobel, C. Rettori and R.D. Zysler, *J. Phys. Chem. C*, **2010**, *114*, 10148.
21. M.E.F. Brollo, R. Lopez-Ruiz, D. Muraca, S.J.A. Figueroa, K.R. Pirota and M. Knobel, *Sci Rep -UK*, **2014**, *4*, 6839.
22. T.D. Nguyen, *Colloids Surf.*, *B*, **2013**, *103*, 326.
23. J.H. Lee, J.T. Jang, J.S. Choi, S.H. Moon, S.H. Noh, J.W. Kim, J.G. Kim, I.S. Kim, K.I. Park and J. Cheon, *Nat. Nanotechnol.*, **2011**, *6*, 418.
24. P. Mendoza Zélis, D. Muraca, J.S. Gonzalez, G.A. Pasquevich, V.A. Alvarez, K.R. Pirota and F.H. Sánchez, *J. Nanopart. Res.*, **2013**, *15*, 1613.
25. D.E. Mihaiescu, A.S. Buteica, J. Neamtu, D. Istrati and I. Mindrila, *J. Nanopart. Res.*, **2013**, *15*, 1857.